

MAGNETIC BRAKING AND FIELD DISSIPATION IN THE PROTOSTELLAR ACCRETION PHASE

D. Galli,¹ M. Cai,² S. Lizano,³ and F. H. Shu⁴

RESUMEN

Damos una reseña del trabajo teórico reciente sobre el papel del campo magnético en el proceso de formación estelar. Primero, nos concentramos sobre la eficiencia del frenado magnético durante el colapso de la nube, y sus consecuencias en la formación de discos mantenidos centrífugamente alrededor de estrellas jóvenes. Luego, relacionamos esto con el conocido problema del flujo magnético en la formación estelar, y mostramos que la introducción de efectos de MHD no ideal es un paso necesario para el desarrollo de modelos autoconsistentes para el colapso de nubes moleculares y la formación y evolución de discos de acreción alrededor de estrellas jóvenes.

ABSTRACT

We summarize recent theoretical work addressing the role of magnetic fields in the process of star formation. First, we concentrate on the efficiency of magnetic braking during cloud collapse and its consequences on the formation of centrifugally supported disks around young stars. Then, we relate this issue to the well-known magnetic flux problem of star formation, and we show that the introduction of non-ideal MHD effects is a necessary step toward the development of self-consistent models for the collapse of molecular clouds and the formation and evolution of accretion disks around young stars.

Key Words: ISM: clouds — ISM: magnetic fields — MHD — planetary systems: protoplanetary disks — stars: formation

1. IDEAL-MHD COLLAPSE OF ROTATING MOLECULAR CLOUD CORES

1.1. *The angular momentum of clouds and disks*

Any realistic calculation of the collapse of a molecular cloud core should include the effects of rotation. In fact, small but detectable levels of rotation have been measured in the outer parts of several cores (see e.g. Goodman et al. 1993; Caselli et al. 2002), with typical values corresponding to angular velocities $\Omega_{\text{cl}} \approx 10^{-14} - 10^{-13} \text{ s}^{-1}$. Although the observed velocity gradients are too small to contribute significantly to the support of the clouds, the dynamical importance of rotation is expected to increase if the angular momentum is conserved during the collapse phase, leading ultimately to the formation of a centrifugally supported circumstellar disk around the accreting protostar (Terebey, Shu, & Cassen 1984).

However, the observations show that the angular momentum of a typical cloud of mass M_{cl} , radius r_{cl} and angular velocity Ω_{cl}

$$J_{\text{cl}} \approx 10^{54} \left(\frac{M_{\text{cl}}}{M_{\odot}} \right) \left(\frac{r_{\text{cl}}}{0.1 \text{ pc}} \right)^2 \times \left(\frac{\Omega_{\text{cl}}}{5 \times 10^{-14} \text{ s}^{-1}} \right) \text{ g cm}^2 \text{ s}^{-1}, \quad (1)$$

is $\sim 1 - 2$ orders of magnitude larger than that inferred for a typical disk of mass M_{d} and radius r_{d} around a star of mass $M_{\star} = M_{\text{cl}}$,

$$J_{\text{d}} \approx 10^{52} \left(\frac{M_{\star}}{M_{\odot}} \right)^{1/2} \left(\frac{r_{\text{d}}}{500 \text{ AU}} \right)^{1/2} \times \left(\frac{M_{\text{d}}}{0.01 M_{\odot}} \right) \text{ g cm}^2 \text{ s}^{-1}. \quad (2)$$

Thus, about 90 to 99% of the angular momentum of a core of a given mass is lost when the same amount of material is transformed into a protostar surrounded by its circumstellar disk. Magnetic braking, often invoked to explain the relatively low rotation rates of cloud cores (Gillis, Mestel, & Paris 1974, 1979; Mouschovias & Paleologou 1979, 1980), may also control the formation and radial extent of circumstellar disks if these are magnetically coupled to an external medium (Contopoulos, Ciolek, & Königl 1998;

¹INAF-Osservatorio Astrofisico di Arcetri, Largo E. Fermi 5, I-50125 Firenze, Italy (galli@arcetri.astro.it).

²Physics Department, National Tsing Hua University, Hsinchu 30013, Taiwan, Republic of China (mike@phys.nthu.edu.tw).

³Centro de Radioastronomía y Astrofísica, Universidad Nacional Autónoma de México, Apdo. Postal 3-72, Morelia, Michoacán 58089, Mexico (s.lizano@astrosmo.unam.mx).

⁴University of California at San Diego, Center for Astrophysics & Space Sciences, 9500 Gilman Drive 0424, La Jolla, CA 92093-0424, USA (fshu@ucsd.edu).

Krasnopolsky & Königl 2002) or to the rest of the collapsing cloud (Allen, Shu, & Li 2003a; Allen, Li, & Shu 2003b).

1.2. Split monopoles and pseudodisks

Recent, semi-analytical calculations and numerical simulations have investigated the evolution of the angular momentum of a collapsing cloud following the increase of density toward the formation of an optically thick core (Tomisaka 2002; Machida et al. 2005a,b; Machida, Inutsuka, & Matsumoto 2006, 2007, 2008) and through the formation of a point-mass into the protostellar accretion phase (Li & Shu 1997; Ciolek & Königl 1998; Allen, Li, & Shu 2003b). Even when the initial state is given appreciable rotation compared to their observational counterparts, accurate simulations of the subsequent evolution assuming field freezing produce no disk formation and no fragmentation. Starting from the seminal work of Allen, Shu, & Li (2003a), and Allen, Li, & Shu (2003b), this result has been confirmed by simulations obtained with smoothed particle magnetohydrodynamics (Hosking & Whitworth 2004; Price & Bate 2007) and adaptive mesh refinement (Ziegler 2005; Fromang, Hennebelle, & Teyssier 2006; Mellon & Li 2008).

Galli et al. (2006) explained the lack of formation of centrifugal disks semi-analytically as being due to the efficient magnetic braking that occurs under field freezing because the collapse of the cloud core into the star traps the corresponding flux and produces a configuration akin to a *split monopole*. In this configuration, the magnetic field is radial and directed in opposite directions above and below the midplane, with intensity (in spherical coordinates)

$$|B_r| = \frac{m_0(1 + H_0)a^3t}{\lambda_*G^{1/2}r^2}, \quad (3)$$

where $m_0 = 0.975$, H_0 is a non-dimensional parameter which measures the overdensity of the initial state with respect to the singular isothermal sphere, a is isothermal sound speed, and λ_* is the non-dimensional mass-to-flux ratio of the split monopole defined as

$$\lambda_* \equiv \frac{2\pi G^{1/2}M_*}{\Phi(r, \pi/2)}. \quad (4)$$

Notice that both the stellar mass, $M_* = m_0(1 + H_0)a^3t/G$, and the flux value at the midplane, $\Phi(r, \pi/2) = 2\pi r^2 B_r$, have no explicit dependence on the radius.

Split monopoles have long lever arms that make magnetic braking very efficient; the resulting outward transport of angular momentum produces a

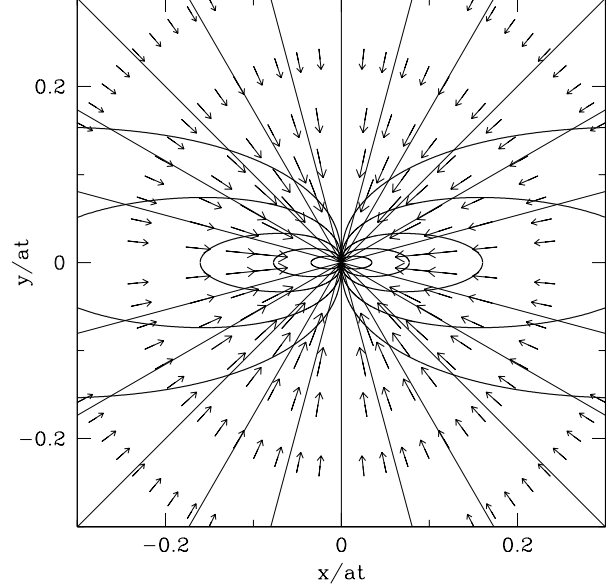


Fig. 1. Inner collapse solutions (valid asymptotically for $r \ll at$) obtained for the collapse of a magnetized singular isothermal toroid with $H_0 = 0.5$ (from Galli et al. 2006). The *heavy solid contours* in each panel are isodensity contours, the *thin solid lines* are the magnetic field lines (which coincide with the streamlines). The *arrows* show the velocity field at different radii.

weak outflow (Tomisaka 2000; Allen, Li, & Shu 2003b), but neither a centrifugally supported disk nor fragmentation into a pair of orbiting binary stars appears. The efficient magnetic braking is due to the field lines that connect the inner region, $r \ll at$, with the rest of the collapsing cloud and thus the magnetic field winding and magnetic braking are calculated self-consistently. Galli et al. (2006) find that in the inner region the collapse becomes quasi-steady, with the magnetic field everywhere parallel to the flow velocity and that the radial component of the field B_r largely dominates over the azimuthal component B_φ , so the winding of the field is never severe. Figure 1 shows the isodensity contours of the “pseudodisk” (Galli & Shu 1993a,b) resulting from the collapse of a magnetized singular isothermal toroid with $H_0 = 0.5$ (Li & Shu 1996), the magnetic field lines of the split monopole at the origin of the coordinate system and the velocity vectors of the infalling gas projected on the meridional plane.

1.3. Catastrophic magnetic braking

Figure 2 shows how the magnetic torque associated with the split monopole field of the central protostar reduces the angular momentum of the infalling gas, constraining the azimuthal velocity to

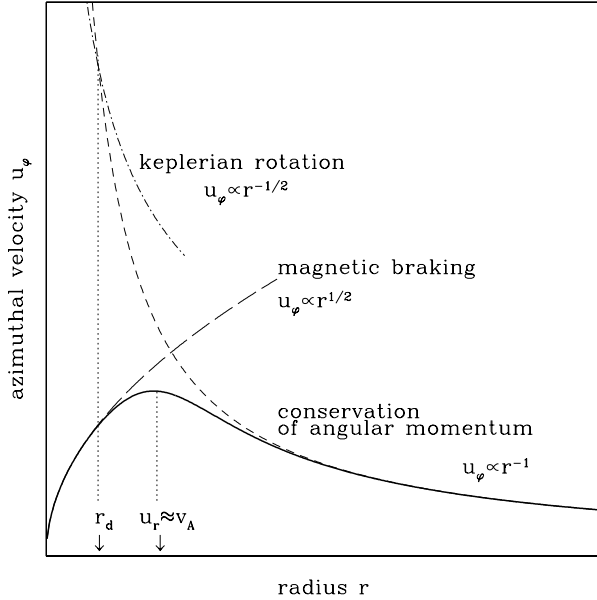


Fig. 2. Schematic behavior of the azimuthal velocity u_ϕ (solid curve) in the equatorial plane of a collapsing cloud as function of the distance r from the central protostar. The radial infall velocity u_r is lower (higher) than the local Alfvén speed v_A inside (outside) the Alfvén radius r_A . In the absence of magnetic braking, conservation of angular momentum results in the formation of a disk of radius r_d .

decrease as $r^{1/2}$ at small radii. Magnetic braking becomes dominant over angular momentum conservation when the infall velocity u_r becomes smaller than the local Alfvén speed v_A inside the Alfvén radius r_A . In contrast, in the absence of magnetic torques, a centrifugally supported disk is formed inside a radius r_d , where the azimuthal velocity increasing as r^{-1} becomes equal to the keplerian velocity around the protostar ($\propto r^{-1/2}$). Thus, magnetic braking during the collapse of an initially rotating and magnetized cloud, under field-freezing, is so strong as to make impossible the formation of centrifugally supported disks for realistic values of the initial magnetic field and rotation speed.

If the magnetic field strength is low enough (or the rotation rate large enough), the formation of a centrifugally supported disk should not be suppressed. More quantitatively, according to Galli et al. (2006), the condition of strong magnetic braking is obtained inside the Alfvén radius r_A , where the infall speed u_r becomes subalfvénic. The Alfvén radius is given approximately by $r_A \approx 2.5\lambda_{cl}^{-2.7} at$, where $\lambda_{cl} = 2\pi G^{1/2}(M_{cl}/\Phi_{cl})$ is the non-dimensional *spherical* mass-to-flux ratio of the parent cloud, whereas the radius of the centrifugally supported disk formed

by a collapsing cloud rotating with uniform velocity $v_0 a$ is $r_d \approx 0.25 v_0^2 at$. The condition for disk formation, $r_d \gg r_A$ then implies $\lambda_{cl} \gg 2.4 v_0^{-0.8}$. This estimate is in qualitative agreement with the results of the detailed collapse calculations of Mellon & Li (2007) and Hennebelle & Fromang (2008) who found disk formation under field-freezing possible only for clouds with $\lambda_{cl} \geq 80$ (for $v_0 \approx 0.5$), or $\lambda_{cl} \geq 20$ (for $v_0 \approx 1$), respectively. The ubiquitous presence of circumstellar disks around young stars and the measured values of $\lambda_{cl} \approx 2$ in molecular clouds (Crutcher 1999) clearly imply that the condition of field-freezing must be violated at some stage during the process of star formation. In the next section we examine how a little bit of field slippage due to electrical resistivity can go a long way toward promoting disk formation.

2. FIELD DISSIPATION DURING GRAVITATIONAL COLLAPSE

2.1. How much flux is brought into a protostar?

There is little doubt that the bulk of the magnetic field threading a core cannot be totally incorporated into the newborn star. The values of $\lambda_\star \approx \lambda_{cl}$ obtained by Galli et al. (2006) for cloud collapse with field-freezing are in dramatic contrast with the measurements of \sim kG fields at the surface of T Tauri stars (Basri, Marcy, & Valenti 1992; Johns-Krull, Valenti, & Koresko 1999), implying $\lambda_{TTauri} \approx 10^4$ or larger⁵. This is a fundamental problem for any theory of star formation: a mass of $\sim 1 M_\odot$ of interstellar material must reduce its magnetic flux by about 3–5 orders of magnitude to become a magnetic star, or by about 8 orders of magnitude to become an ordinary star like the Sun. This *magnetic flux problem* was already recognized by Mestel & Spitzer (1956).

Assuming quasi-steady state and a spatially uniform resistivity coefficient η , Shu et al. (2006) solved the problem of magnetic field dissipation during the accretion phase of star formation and computed the resulting magnetic-field configuration when one adopts a kinematic approximation (that ignores the back reaction of the changed magnetic topology on the flow) to solve the induction equation. In steady state, with magnetic flux advection balanced by field dissipation, the induction equation takes the form

$$\mathbf{u} \cdot \nabla \Phi = \eta S^2(\Phi), \quad (5)$$

⁵Since the fields measured in T Tauri stars are probably generated by internal dynamo action, the discrepancy is even more severe than “merely” a factor of 10^4 .

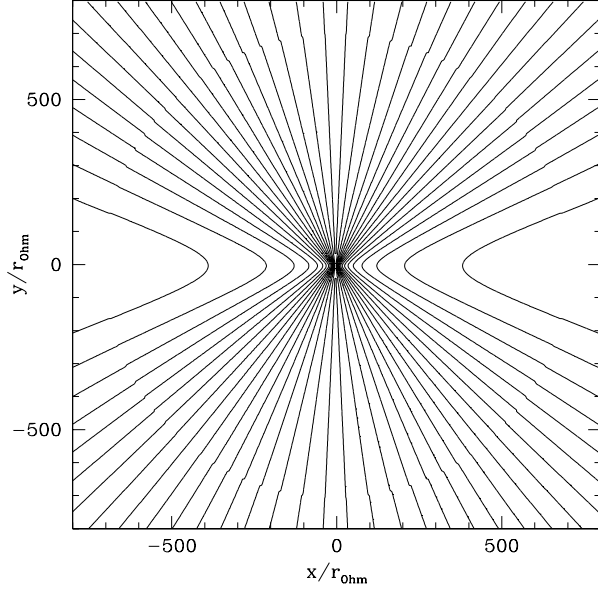


Fig. 3. At large distances from the accreting protostar, the magnetic field lines are asymptotically radial, and the field approaches a split-monopole configuration with non-dimensional mass-to-flux ratio λ_* .

where Φ is the magnetic flux and S^2 is the second-order differential operator

$$S^2 = \frac{\partial^2}{\partial r^2} + \frac{1}{r^2} \frac{\partial^2}{\partial \theta^2} - \frac{\cot \theta}{r^2} \frac{\partial}{\partial \theta}. \quad (6)$$

In this specific context, the induction equation must be solved under two boundary conditions: (i) the condition that the magnetic flux accreted by the central star is zero at any time (motivated by the observational evidence that $\lambda_{cl} \ll \lambda_{T \text{ Tauri}}$), and (ii) the condition that the magnetic field at infinity asymptotically approaches that of a split monopole with mass-to-flux ratio λ_* (to recover the inner limit of the field-freezing solution discussed in the previous section). Thus, in the language of matched asymptotic expansions, the results of Galli et al. (2006) and Shu et al. (2006) represent the outer and inner solutions, respectively, of a *global* solution of the equations of non-ideal MHD for the accretion phase of star formation, with the resistivity η playing the role of the small parameter associated to the highest spatial derivatives. The solution of equation (6) for the flux function Φ can be obtained *analytically* as a series of products of Legendre polynomials for the angular part and confluent hypergeometric functions of the first kind for the radial part. In this solution, the morphology of the magnetic field changes from almost radial at large distances (see Figure 3) to asymptotically straight and uniform with intensity

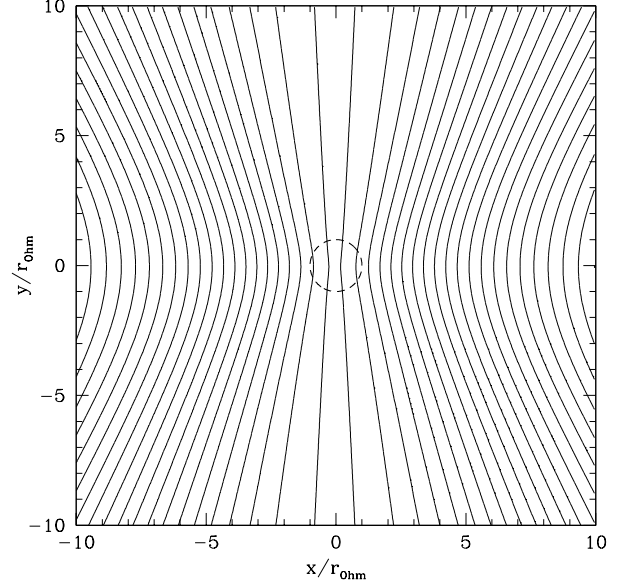


Fig. 4. Same magnetic field lines as in Figure 2 in the inner regions close to the accreting protostar. Within the Ohm's radius (*dashed circle*), magnetic field dissipation enforces an almost straight and uniform magnetic field.

B_c in the innermost regions (see Figure 4), where magnetic reconnection prevents the formation of a split monopole and its associated large electrical currents, a process first analyzed in this context by Mestel & Strittmatter (1967).

2.2. The Ohm radius

To determine the value of the resistivity coefficient η , we have considered the restrictions imposed by measurements of magnetic fields in meteorites and the magnetic field configuration around protostars inferred from high-resolution sub-mm polarization observations (Girart, Rao, & Marrone 2006; Gonçalves, Galli, & Girart 2008). These constraints require an effective resistivity $\eta \approx 10^{20} \text{ cm}^2 \text{ s}^{-1}$, at least one order of magnitude larger than the microscopic electric resistivity of the infalling gas (Nakano, Nishi, & Umebayashi 2002; Desch & Mouschovias 2001). An “anomalous” source of magnetic diffusivity may be required, which could be turbulent in its origin (see, e.g., Cattaneo & Vainshtein 1991; Lazarian & Vishniac 1999; Kim & Diamond 2001; Lazarian, Vishniac, & Cho 2004).

The dissipation of the magnetic field occurs inside a region of radius r_{Ohm} , which is inversely proportional to the instantaneous stellar mass M_* , and

proportional to the square of the electrical resistivity,

$$\begin{aligned} r_{\text{Ohm}} &= \frac{\eta^2}{2GM_\star} \\ &\approx 10 \left(\frac{\eta}{10^{20} \text{ cm}^2 \text{ s}^{-1}} \right)^2 \left(\frac{M_\star}{M_\odot} \right)^{-1} \text{ AU} \end{aligned} \quad (7)$$

the so-called ‘‘Ohm’s radius’’. The relation between the field strength B_c at the center, the spatial extent $\sim r_{\text{Ohm}}$ where the field is approximately uniform, the instantaneous stellar mass, and the value of the electrical resistivity is given by

$$\begin{aligned} B_c &= \frac{4G^{5/2} M_\star^3}{15\lambda_\star \eta^4} \\ &\approx 25 \lambda_\star^{-1} \left(\frac{M_\star}{M_\odot} \right)^3 \left(\frac{\eta}{10^{20} \text{ cm}^2 \text{ s}^{-1}} \right)^{-4} \text{ G} \end{aligned} \quad (8)$$

showing that B_c scales with the electric conductivity σ and stellar mass as $\sigma^4 M_\star^3$, a result that may have interesting consequences for high-mass stars.

2.3. The mass-to-flux ratio of a disk

The results of Shu et al. (2006), combined with observational data on the morphology of the magnetic field around young stars, suggest that, for realistic values of η , the magnetic flux trapped in a circumstellar disk of radius r_d around a star of mass M_\star is only a factor of a few smaller than the flux that would be trapped, under field-freezing, in a split monopole concentrated in a protostar of the same mass and the same magnetic field at large distances. Figure 5 shows the mass-to-flux ratio λ normalized to the mass-to-flux ratio λ_\star of the split monopole for the model shown in Figures 2 and 3 as a function of the distance from the protostar. For values of the Ohm radius of 1, 10 and 100 AU, the mass-to-flux ratio of a typical disk of radius, say, $r_d = 500$ AU around a protostar of mass M_\star is higher by a factor of 1.5, 2.5 and 10.5 than that of the split monopole configuration. Taking $r_d = 500$ AU and $\lambda_{\text{cl}} \approx 2$ as fiducial values, the mass-to-flux ratio of a typical circumstellar disk is expected to be $\lambda_d \approx 3$ for $r_{\text{Ohm}} = 1$ AU and $\lambda_d \approx 5$ for $r_{\text{Ohm}} = 10$ AU, respectively. The net magnetization of circumstellar disks resulting from interstellar fields dragged in by the process of gravitational collapse makes the magnetorotational instability (Hawley & Balbus 1991; Balbus & Hawley 1998) a natural candidate for the mechanism of inward transport of matter and outward transport of angular momentum, with important implications for disk winds, X-winds, and funnel flows (Shu et al. 2007).

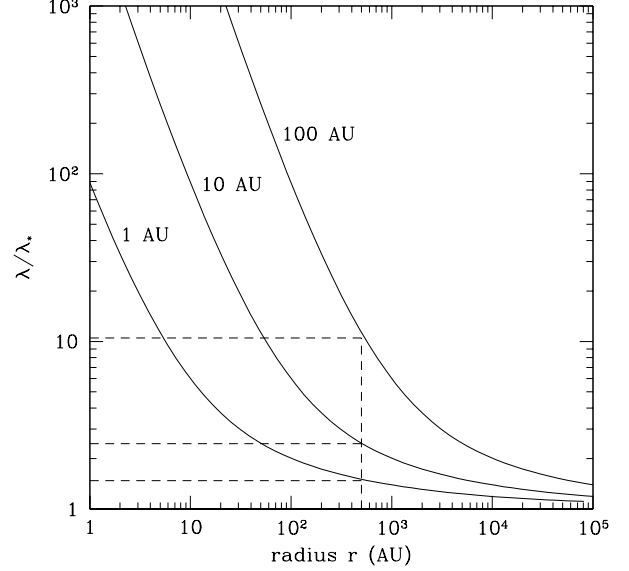


Fig. 5. Non-dimensional mass-to-flux ratio λ normalized to the mass-to-flux ratio λ_\star of a split monopole with the same field at infinity, as function of the distance r from the protostar for the non-ideal MHD collapse model of Shu et al. (2006). The three curves are for $r_{\text{Ohm}} = 1, 10$ and 100 AU. The *dashed lines* indicate likely values of λ/λ_\star for a disk with radius $r_d = 500$ AU.

2.4. Joule heating

Finally, the magnetic energy annihilated by the process of field dissipation per unit time and unit volume (Joule heating rate) in the innermost region is approximately given by

$$\begin{aligned} \dot{\mathcal{E}} &\approx \frac{8G^4 M_\star^5}{675 \lambda_\star^2 \eta^5} \\ &\approx 300 \lambda_\star^{-2} \left(\frac{M_\star}{M_\odot} \right)^5 \left(\frac{\eta}{10^{20} \text{ cm}^2 \text{ s}^{-1}} \right)^{-5} L_\odot. \end{aligned} \quad (9)$$

With our fiducial values we obtain $\dot{\mathcal{E}} \approx 3 L_\odot$, but given the sensitive dependence of $\dot{\mathcal{E}}$ on the uncertain parameter η this number may not be very significant. What is more interesting is that the adopted resistivity, which is high by conventional microscopic standards, cannot be much lower without violating observational constraints concerning the total luminosity from regions of low-mass star formation (see the reviews of Evans 1999 or Lada & Lada 2003).

3. SUMMARY

The analytical results summarized in this paper confirm and explain the trend emerging from several numerical simulations addressing the phase of collapse of molecular cloud cores with realistic values

of rotation and magnetization: with field-freezing, magnetic braking prevents the formation of centrifugally supported disks and cloud fragmentation. Non-ideal MHD effects leading to field dissipation must occur prior or simultaneously to the formation of the disk ($r_{\text{Ohm}} \sim r_{\text{d}}$), and need to be incorporated in realistic models. Having shown that a spatially uniform resistivity (although higher in magnitude than the standard collisional value) can dissipate enough magnetic field so as to solve the magnetic flux problem satisfying the available observational constraints, one now needs to solve the full dynamic problem of magnetic field dissipation and formation of a centrifugally supported protoplanetary disk in a self-consistent way. The simulations of Machida, Inutsuka, & Matsumoto (2006, 2007, 2008) represent an important step in this direction.

REFERENCES

- Allen, A., Shu, F. H., & Li, Z.-Y. 2003a, *ApJ*, 599, 351
 Allen, A., Li, Z.-Y., & Shu, F. H. 2003b, *ApJ*, 599, 363
 Balbus, S. A., & Hawley, J. F. 1998, *Rev. Mod. Phys.*, 70, 1
 Basri, G., Marcy, G., & Valenti, J. 1992, *ApJ*, 390, 622
 Caselli, P., Benson, P., Myers, P. C., & Tafalla, M. 2002, *ApJ*, 572, 238
 Cattaneo, F., & Vainshtein, S. I. 1991, *ApJ*, 376, 121
 Ciolek, G. E., & Königl, A. 1998, *ApJ*, 504, 257
 Contopoulos, I., Ciolek, G. E., & Königl, A. 1998, *ApJ*, 504, 247
 Crutcher, R. 1999, *ApJ*, 520, 706
 Desch, S. J., & Mouschovias, T. Ch. 2001, *ApJ*, 530, 314
 Evans, N. J. 1999, *ARA&A*, 37, 311
 Fromang, S., Hennebelle, P., & Teyssier, R. 2006, *A&A*, 457, 371
 Galli, D., & Shu, F. H. 1993a, *ApJ*, 417, 220
 ———. 1993b, *ApJ*, 417, 243
 Galli, D., Lizano, S., Shu, F. H., & Allen, A. 2006, *ApJ*, 647, 374
 Gillis, J., Mestel, L., & Paris, R. B. 1974, *Ap&SS*, 27, 167
 ———. 1979, *MNRAS*, 187, 311
 Girart, J. M., Rao, R., & Marrone, D. P. 2006, *Science*, 313, 812
 Gonçalves, J., Galli, D., & Girart, J. M. 2008, *A&A*, 490, L39
 Goodman, A. A., Benson, P. J., Fuller, G. A., & Myers, P. C. 1993, *ApJ*, 406, 528
 Hennebelle, P., & Fromang, S. 2008, *A&A*, 477, 9
 Hawley, J. F., & Balbus, S. A. 1991, *ApJ*, 381, 496
 Hosking, J. G., & Whitworth, A. P. 2004, *MNRAS*, 347, 3
 Johns-Krull, C. M., Valenti, J., & Koresko, C. 1999, *ApJ*, 516, 900
 Kim, E., & Diamond, P. H. 2001, *ApJ*, 556, 1052
 Krasnopolsky, R., & Königl, A. 2002, *ApJ*, 580, 987
 Lada, C. J., & Lada, E. 2003, *ARA&A*, 41, 57
 Lazarian, A., & Vishniac, E. T. 1999, *ApJ*, 517, 700
 Lazarian, A., Vishniac, E. T., & Cho, J. 2004, *ApJ*, 606, 180
 Li, Z.-Y., & Shu, F. H. 1996, *ApJ*, 472, 211
 ———. 1997, *ApJ*, 475, 237
 Machida, M. N., Matsumoto, T., Tomisaka, K., & Hanawa, T. 2005, *MNRAS*, 362, 369
 Machida, M. N., Matsumoto, T., Hanawa, T., & Tomisaka, K. 2005, *MNRAS*, 362, 382
 Machida, M. N., Inutsuka, S., & Matsumoto, T. 2006, *ApJ*, 647, L151
 ———. 2007, *ApJ*, 670, 1198
 ———. 2008, *ApJ*, 676, 1088
 Mellon, R., & Li, Z.-Y. 2008, *ApJ*, 681, 1356
 Mestel, L., & Spitzer, L. 1956, *MNRAS*, 116, 503
 Mestel, L., & Strittmatter, P. A. 1967, *MNRAS*, 137, 95
 Mouschovias, T. Ch., & Paleologou, E. V. 1979, *ApJ*, 230, 204
 ———. 1980, *ApJ*, 237, 877
 Nakano, T., Nishi, R., & Umebayashi, T. 2002, *ApJ*, 573, 199
 Price, D. J., & Bate, M. R. 2007, *MNRAS*, 337, 77
 Shu, F. H., Galli, D., Lizano, S., & Cai, M. 2006, *ApJ*, 647, 382
 Terebey, S., Shu, F. H., Cassen, P. 1984, *ApJ*, 286, 529
 Tomisaka, K. 2000, *ApJ*, 528, L41
 Ziegler, U. 2005, *A&A*, 435, 385